Research Article
Open Access

Biomechanical evaluation of a full-length (T12-S) synthetic lumbar spine model

Abstract

Cadaveric tissue-based testing is the standard method for biomechanically evaluating spinal instrumentation. Synthetic lumbar spine models have been developed and are commercially available as a cost saving alternative to human tissue. Validation studies have been done on single lumbar motion segment units (MSU) and partial synthetic lumbar models. A full-length synthetic lumbar spine model (T12 to sacrum) has become available that can serve as an alternative to tissue, but the biomechanical structural properties are not available. Additional kinematic parameters (like center of rotation (COR) and instantaneous axes of rotation (IAR)) also do not exist. The objectives of this study were to determine the flexion/extension stiffness properties of a full-length synthetic lumbar spine model and to define the segmental and global kinematic parameters. The synthetic lumbar model was mounted in a robotic testing platform and tested using pure moment loads and 20N axial compression between 25° flexion and 10° extension. Global position of each vertebra was measured and used to calculate the global COR and global and local IAR values of each MSU. Rotational stiffness, global COR, and local and global IAR parameters were calculated every 2° change in 0.5° increments. MSU rotational responses were normalized to the total rotation and expressed as a percent contribution (%Rot). All spinal levels were involved in contributing to the overall motion and the %Rot was within 2 standard deviations of similar rotational data sets from *in vivo* studies and *in vitro* tests on cadaveric spines. The CORs of each MSU were located near the mid-point of their respective IAR path. Global IAR paths were approximately mid-distance between the respective spinal level and the fixed sacral body. The biomechanical properties of the full-length synthetic lumbar model were comparable to *in vivo* and *in vitro* studies supporting its use in other testing applications.

Keywords: biomechanical testing, lumbar spine, synthetic model, spinal kinematics

Volume 3 Issue 3 - 2019

Denis J DiAngelo, Daniel S Hoyer, Chloe L Chung
Department of Orthopedic Surgery and Biomedical Engineering, University of Tennessee Health Science Center, USA

Correspondence: Denis J DiAngelo, PhD, Department of Orthopaedic Surgery and Biomedical Engineering, The University of Tennessee Health Science Center, 956 Court Ave, Suite E226, Memphis, TN 38163, USA,
Email ddiangelo@uthsc.edu

Received: June 17, 2019 | **Published:** June 24, 2019

Abbreviations: COR, center of rotation; IAR, instantaneous axis of rotation; MSU, motion segment unit; 2D, two dimensional; %Rot, percent contribution

Introduction

Cadaveric tissue-based testing is the standard method for biomechanically evaluating spinal instrumentation in the lumbar spine.[1,2] In general, the motion response of each spinal segment is measured in response to a known loading condition. Application of pure moment loads is the most common method,[2,3] and can also be modified with the addition of a compressive follower load,[4,5] or in combination with compression and/or shear forces.[6,7] More recently, multi-body synthetic lumbar spine models have been developed and are commercially available as a cost saving alternative to human cadaveric tissue [Sawbones Inc., Pacific Research Laboratories, Vashon, WA]. The original validation studies of these synthetic models were done on either a single lumbar segment (L3-L4) model,[8–11] or various multi-level lumbar models.[12,13] Camisa et al. validated the flexion/extension, lateral bending, and axial rotation flexibility properties of a L1-L5 model against human cadaveric tissue tested under pure moment loading conditions.[13] Range of motion data were comparable to cadaveric specimens. Wang et al. studied the anatomical and biomechanical flexibility properties of a single L3-L4 synthetic lumbar model and also found no differences with human cadaveric data in the literature.[11] The model was further used by Wang et al. to compare different spinal fusion instrumentation under cyclic pure moment load endurance testing.[14]

More recently, a full-length synthetic analog lumbar spine model (T12-sacrum) has become available for testing long multi-segment spinal constructs (Product #3430, Sawbones Inc., Pacific Research Laboratories, Vashon, WA). Although these models can be used as an alternative method to tissue-based testing of spinal fusion instrumentation,[13,14] we have an interest to incorporate this full lumbar model into a testing protocol for biomechanically analyzing lower back support devices.[15] Regardless of the application, information of the rotational stiffness (angle versus moment) properties for this full lumbar synthetic model are not available. Additional kinematic parameters (like the center of rotation (CoR) and instantaneous axes of rotation (IAR)) will provide further biomechanical description of these devices. However, information of the IAR or CoR parameters for any of the synthetic lumbar spine models from Sawbones Inc. does not exist.

The CoR of lumbar spinal segments is typically calculated from the end range positions of the adjacent vertebrae while the IAR describes the moving path of the spinal segment using the positional changes of two fixed points on a rigid body.[16–24] The Reuleaux method is the most common technique used to calculate the IAR but is affected by the accuracy of the measurement system. To combat this, Crisco et al.,[25] proposed a refinement to the Reuleaux method to reduce the error in the IAR calculation process, which was implemented in this study. The objectives of this study were to determine the flexion/extension flexibility properties of a full-length (T12-sacrum) synthetic lumbar spine model and to define the segmental and global kinematic parameters of each vertebral level of the model. The full-length synthetic lumbar spine model was tested under pure moment loading conditions and a modified version of Crisco's technique was developed to determine the global and local/segmental CoR and IAR kinematic parameters after the spinal segments were isolated into adjacent pairs. The long-term use for this synthetic spine model is to

support the development of a standardized testing methodology for evaluating and designing lumbar spinal orthoses. In summary, this paper describes a new mathematical approach to determine the CoR and IAR parameters of a multi-level spine model using commonly measured spatial data of each vertebral segment. The technique was then used to describe these kinematic parameters for a new commercially available full length synthetic lumbar spine model. Additionally, standard pure moment biomechanical tests were carried out to quantify segmental motion and rotational stiffness properties of the synthetic model that were compared to *in vivo* and *in vitro* findings for validation purposes.

Materials and methods

Synthetic lumbar spine model and testing platform

A full-length (T12/S1) synthetic lumbar spine model (SKU#3430, Sawbones Inc., Pacific Research Laboratories, and Vashon, WA) was obtained with simulated intervertebral discs, vertebrae and ligaments. A photograph and schematic of the complete synthetic model are shown in Figure 1 and had potted blocks affixed to both ends.

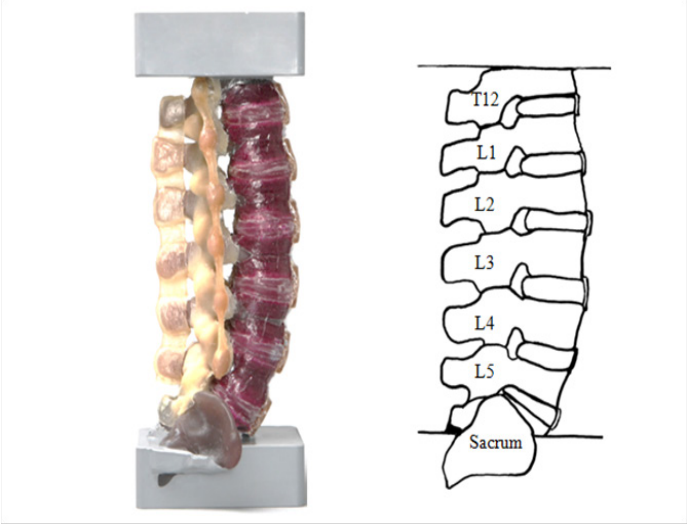

Figure 1 A) Synthetic Lumbar Spine Model and B) Schematic Representation of Lumbar Spine Model. The sacrum served as the origin of global CoR and IAR parameters.

Kinematic analysis

The planar two-dimensional (2D) motion of each vertebral body of the model was measured using a camera-based system consisting of a receiver unit (two planar charge-coupled device [CCD] cameras) and active light-emitting diode (LED) targets (operating at near infrared light). An array of two LED targets, separated by 3 inches, were attached rigidly to each vertebral level (Figure 2). The location of the array in three-dimensional space uniquely determined the global position of each vertebra with respect to a fixed reference frame (*i.e.,* the receiver unit) that was transferred to the sacrum using principles of rigid body mechanics. Local vertebral motion was expressed relative to the subjacent vertebral body using the equations and methods described below. A modified version of the Reuleaux method as proposed by Crisco et al.,[25] was used to calculate the CoR and IAR parameters.

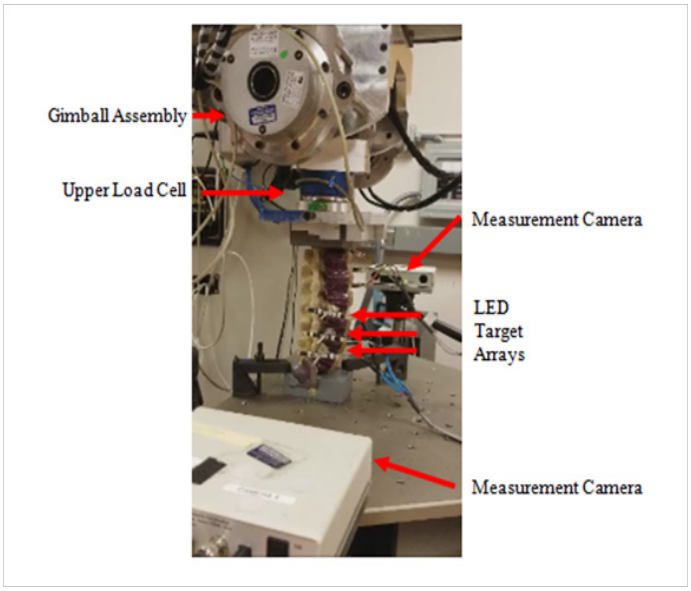

Figure 2 Experimental Set-up of Synthetic Lumbar Spine Mounted in Robotic Testing Platform.

Method for analyzing multi-level spine model segmentally

In order to determine the local IAR of each spinal level, two adjacent spinal bodies were isolated from the full spine model. The motion of the spinal segment's upper body (UB) had to be expressed relative to the stationary lower body (LB) by negating all translational and rotational changes due to the motion of the lower body from both the UB and LB. Figure 3 and the following equations define the method. The known (global) locations of each body are relative to the sacrum target array after being transferred from the reference frame of the camera. First, a vector $UB_{2'}$ was defined as the spatial position of the UB at time point 2 due to the motion of the lower body alone (i.e., as if the UB was rigidly attached to the LB). The spatial position (cartesian coordinates of x and y) of $UB_{2'}$ was calculated using Equations 1A-C below. This location was expressed as the sum of the starting linear position of the UB at time 1 and the linear displacement of the LB between time points 1 and 2, minus the linear displacement of the UB due to the rotation of the LB between time points 1 and 2.

Eq. 1

$$1A.\ \overline{\Delta_{12}LB} = \overline{LB_2} - \overline{LB_1}$$

$$1B.\ \overline{UB_{2'}}(x) = \overline{UB_1}(x) + \overline{\Delta_{12}LB}(x) - L*\left[\cos(\beta_1) - \cos(\beta_2)\right]$$

$$1C.\ \overline{UB_{2'}}(y) = \overline{UB_1}(y) + \overline{\Delta_{12}LB}(y) - L*\left[\sin(\beta_1) - \sin(\beta_2)\right]$$

$$Where\ \beta_1 = \tan^{-1}\left(\frac{UB_1(y) - LB_1(y)}{UB_1(x) - LB_1(x)}\right)\ and\ \beta_2 = \beta_1 + \Delta_{12}LB(\theta)$$

The angular (Θ) or rotational position $UB_{2'}$ was calculated using Equation 2 below. The angle of $UB_{2'}$ was expressed as the sum of the angular position of the UB at time point 1 and the angular displacement of the LB between time points 1 and 2.

Citation: DiAngelo DJ, Hoyer DS, Chung CL. Biomechanical evaluation of a full-length (T12-S) synthetic lumbar spine model. *MOJ App Bio Biomech.* 2019;3(3):70–75. DOI: 10.15406/mojabb.2019.03.00106

Eq. 2

$$UB_{2'}(\theta) = UB_1(\theta) + \Delta_{12}LB(\theta)$$

Finally, a second vector $UB_{2''}$ was defined as the spatial position of UB at time point 2 due to the motion of the UB alone (i.e., the effects of the motion of the LB are negated). $UB_{2''}$ was calculated using Equations 3A-B below. The position of $UB_{2''}$ is calculated using the known position of UB_2 minus the computed position of $UB_{2'}$, plus the known starting position of UB_1,

Eq. 3

$$3A.\ \overline{\Delta_{2-2'}UB}(x,y,\theta) = \overline{UB_2}(x,y,\theta) - \overline{UB_{2'}}(x,y,\theta)$$

$$3B.\ \overline{UB_{2''}}(x,y,\theta) = \overline{UB_1}(x,y,\theta) + \overline{\Delta_{2-2'}UB}(x,y,\theta)$$

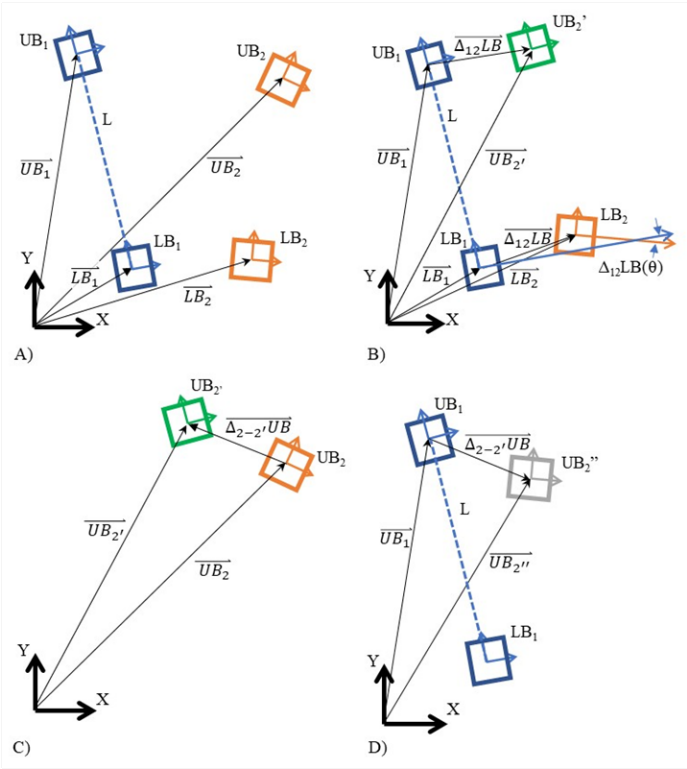

Figure 3 Method for determining the local IAR of upper body (UB) relative to the lower body (LB). A) UB_1 is a known location of Upper Body at time 1, UB_2 is a known location of Upper Body at time 2, LB_1 is a known location of Lower Body at time 1, LB_2 is a known location of Lower Body at time 2, B) $UB_{2'}$ is a calculated location of Upper Body at time 2 due to the motion of Lower Body alone, C) The relative change of the UB between $UB_{2'}$ and the final position UB_2 is given by Δ2-2'UB, and D) $UB_{2''}$ is a calculated location of Upper Body at time 2 due the motion of Upper Body alone relative to a stationary LB.

These calculations were repeated incrementally every 0.5 degree to determine a new path of motion for UB relative to a fixed LB reference frame so that Crisco's equations[25] could be used to calculate the local CoR and IAR parameters segmentally across the different levels of the synthetic spine. The global IAR values of each spinal segment was calculated every 2 degrees change in 0.5 degree increments (i.e., 0-2, 0.5-2.5, 1.0-3.0, etc).

Testing protocol

The synthetic spine model was mounted in a robotic testing platform[26] that had four programmable degrees of freedom with a positional resolution of 2 µm in x, 0.31µm in z, and 0.0002° about y (Figure 2). An upper load cell (ULC) (JR3 Inc., Woodland, CA) with 400N load and 40Nm moment capacities was attached to the gimbal assembly and measured the forces and moment applied to the spine model at a rate of 15Hz. The spine model was tested under a pure moment and an axial load of 20N was applied to the spine[27] and rotated between 25° flexion and 10° extension at 1.6°/s. Motion in either direction was stopped if the moment limit exceeded 10Nm. The axial load was applied through the global point of rotation of the entire spine model (i.e., point of rotation of T12 relative to the sacrum). This step minimized any off-axis bending moment from being created by the axial load. The control strategy has been validated and used in other biomechanical studies.[15,27–29]

Data management

The global stiffness of the synthetic spine model was expressed as a function of the applied moment relative to the overall global rotation. The position data of each vertebral body were measured at 10Hz and used to determine the local and global IAR and CoR parameters. Noise in the camera data was filtered out using a curve fitting approach. The rotational response of each MSU level was normalized to the total rotation of the synthetic spine model and expressed as a percent contribution (%Rot). Similar rotational data sets from both *in vivo* studies[30-35] and *in vitro* pure moment tests,[7,36,37] on cadaveric (L1-S1) lumbar spines were compiled for comparison purposes.

Results

Global stiffness and MSU rotational contribution

The flexion and extension moment – rotation data of each vertebral level of the synthetic model is shown in Table 1. The spine model reached 25° flexion at a moment of 7.4Nm and 10° extension at a moment of 6Nm. However, since only validation data for the L2-L5 synthetic models exists in the Sawbones literature,[12] the equivalent segment data from the full-length synthetic spine model was extracted and compared. The corresponding stiffness curve in Figure 4 shows the similarity between the two data sets. To further validate the structural properties of the full-length synthetic model, the rotational response of each vertebral level of the full-length (T12-S1) model was normalized to the total lumbar spine rotation and compared to similar *in vivo* and *in vitro* data sets found in the literature. Figure 5 compares the percent motion contribution of the synthetic model to three human cadaveric data sets[7,36,37] tested under similar pure moment loading conditions, while Figure 6 compares the full-length data to five *in vivo* studies.[30–35] No statistical analysis was performed, as data from only one full-length analog spine was available for comparison. However, as illustrated in Figures 5 & 6, all spinal levels were involved in contributing to the overall motion response regardless of the testing method (i.e., *in vitro*, *in vivo*, or synthetic model), and a close match was found at the three upper motion segment units. The mean and standard deviation of the three pure moment *in vitro* studies was added to Figure 5 and the mean and standard deviation of the five *in vivo* studies was added to Figure 6. The %Rot of all MSU levels was within 2 standard deviations for either test comparison.

Global CoR and IAR patterns

The global path of the instant axis of rotation of each vertebral body relative to a fixed sacrum reference frame is shown in Figure 7 for the full sweep of motion from 10° extension to 25° flexion. The transition point defining neutral orientation (0°) is also included. The

Citation: DiAngelo DJ, Hoyer DS, Chung CL. Biomechanical evaluation of a full-length (T12-S) synthetic lumbar spine model. *MOJ App Bio Biomech.* 2019;3(3):70–75. DOI: 10.15406/mojabb.2019.03.00106

IAR path of the upper four vertebral bodies was located in the mid-region of the bodies and transition downward during flexion, while the IAR of the lower two (L4 and L5) vertebral bodies transitioned to a horizontal path that moved posteriorly during flexion. Minimal translation of the IAR path occurred during extension. When looking at the relative location of the IAR path for each body relative to the fixed reference frame of the sacrum, the path was located close to the mid-distance of each body relative to the sacral body. That is, the IAR path of T12 body was located within the L3 body, starting at the top surface and moved downward, which is about half the distance between the T12 and S1 bodies. The location of the global IAR paths of the other vertebral bodies was similarly located close to the mid-distance between the respective vertebral body and the fixed sacral body.

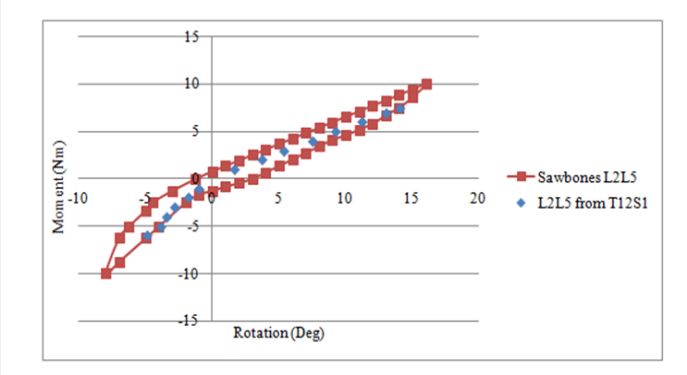

Figure 4 Comparison of Moment-Rotation Stiffness Properties between L2-L5 Sawbone's Inc. Model[12] and Segments L2-L5 of the New Untested Full-length (T12-Sacrum) Model.

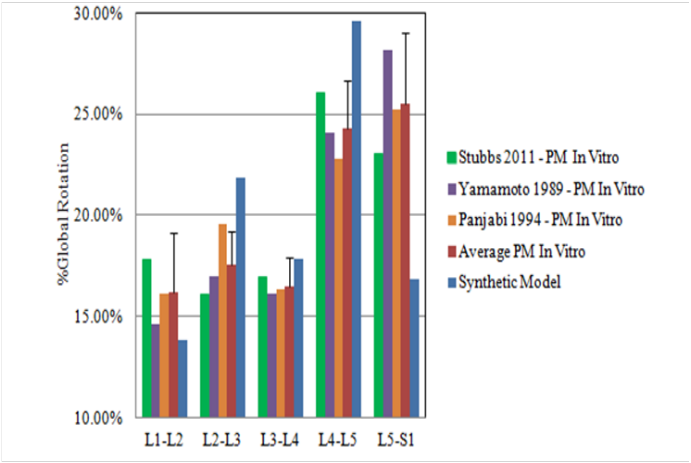

Figure 5 Comparison of Percent Global Segmental Motion Response between Synthetic Model and *In Vitro* Pure Moment Test Results.[7,36,37]

Local CoR and IAR patterns

The local IAR path of each vertebral body relative to its subjacent body is shown in Figure 8. For all MSUs, the local IAR paths were generally located along the superior endplate surface of the lower body. The local IAR of the upper two MSU (T12-L1 and L1-L2) was near the posterior wall of the endplate surface while the local IAR locations of the remaining vertebrae were closer the midline of the end plate surface of the lower vertebral body. The profile of each MSU path is largely dictated by the mechanical properties of the interconnecting vertebral disc material and pseudo-ligament structures. The CoR values of each MSU are also shown on Figure 8 and were located near the mid-point of their respective IAR path. For those MSU with their CoR located near the midline of the vertebral disc, involvement of the facet joints was likely minimal.

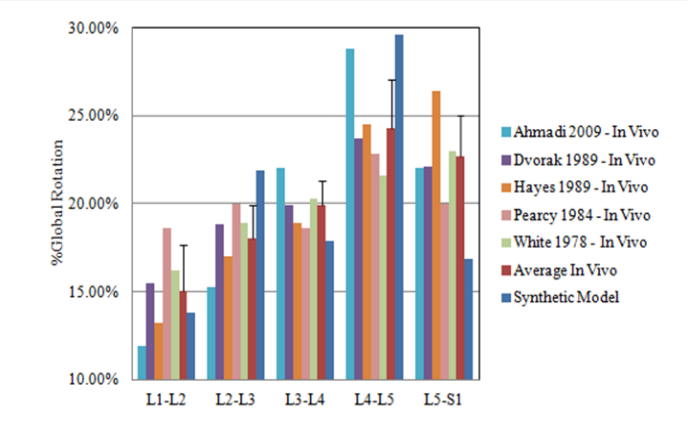

Figure 6 Comparison of Percent Global Segmental Motion Response between Synthetic Model and *In Vivo* Motion Patterns.[30–35]

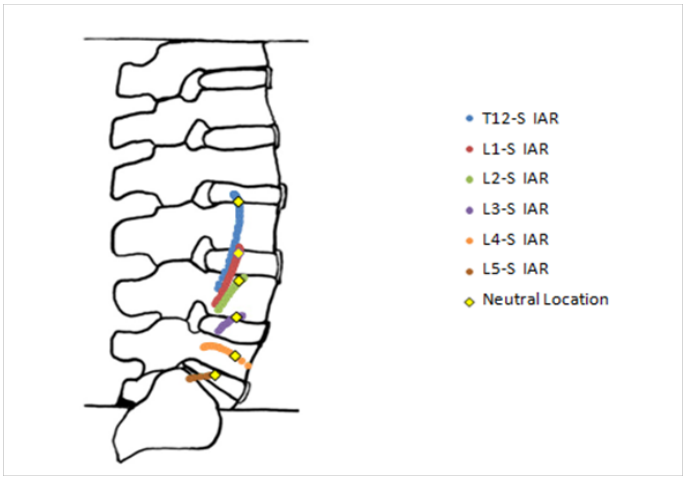

Figure 7 Global IAR Patterns of Each Spinal Level.

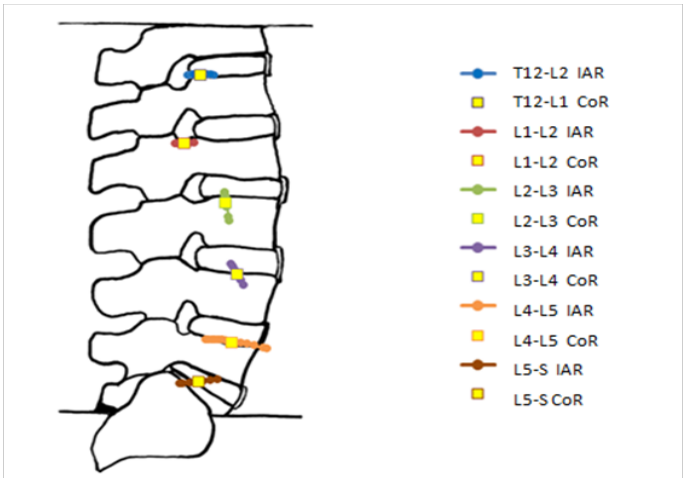

Figure 8 Local CoR and IAR Patterns of Each Motion Segment Unit.

Citation: DiAngelo DJ, Hoyer DS, Chung CL. Biomechanical evaluation of a full-length (T12-S) synthetic lumbar spine model. *MOJ App Bio Biomech.* 2019;3(3):70–75. DOI: 10.15406/mojabb.2019.03.00106

Table 1 Flexion and Extension Response per Motion Segment Unit

Motion Segment Unit	Flexion (Deg) at 7.4Nm	Extension (Deg) at 6Nm
T12-L1	5.4	1.5
L1-L2	2.3	1.5
L2-L3	4.5	1.5
L3-L4	3.3	1.5
L4-L5	6.3	1.5
L5-S1	3.3	1.6
T12-S1	25.1	9.1

Discussion

A unique set of biomechanical data describing the performance of a new commercially available full-length synthetic model of the lumbar spine is provided. However, before such models can be considered as an alternative material to human cadaveric tissue, validation of their mechanical properties is required. The global stiffness property was comparable to published *in vitro* findings found in the literature[7,36,37] when tested under similar loading conditions. Similarly, the involvement of each motion segment was comparable to rotational patterns observed during *in vivo* flexion and extension activities. Since the published segmental rotations of L2-L5 model,[12] were within one standard deviation of human cadaveric tissue, and the response of the full-length synthetic model was comparable to them, the full-length synthetic model can also be considered an adequate representation of human tissue. Further, in addition to establishing the biomechanical properties of the synthetic lumbar spine, a method was established to determine the local paths of the CoR of each MSU. This method can easily be implemented by other researchers capturing global positional data of each vertebral body. For the synthetic lumbar spine model, the locations of the local CoR were close to the midline of the superior end plate of the lower subjacent body. Other researchers have also analyzed the IAR and CoR of the lumbar spine. Gertzbein et al.,[17] biomechanically tested five human cadaveric L4-L5 segments and reported a locus of IAR points in the posterior half of the intervertebral disc region, while Haher et al.,[18] found the IAR of a single L4-L5 segment to be in the vicinity of the facet joints. However, many of the earlier studies, similar to Gertzbein et al.,[17] and Haher et al.,[18] had methodological differences that limited direct comparison or validation to them.

Pearcy et al.,[21] carried out one of the first *in vivo* studies measuring the IAR of the lumbar spine that addressed many of the potential error problems inherent with the measurement process itself. The mean location of the IAR positions for 10 subjects was close to the midline of the lumbar spine near the superior endplate of the lower vertebral body very similar to the IAR locations of the synthetic lumbar spine. Inoue et al.,[20] carried out a biomechanical study on five deer L5-L6 segments to determine the effects of spinal instrumentation on the location of the IAR for different planes of motion, including the sagittal plane. Although the deer specimen differs from the human cadaver spine, the location of the IAR was in the region of the spinal cord, similar to L1-L2 segment of the synthetic spine. Of interest with their study was the method used to determine the IAR, which was similar to the approach used here. More recent work by Bifulco et al.,[38] used advanced video fluoroscopy methods to sequentially measure the IAR of a L2-L3 segment on the human subjects. The mean location of the IAR path was in the lower L3 vertebral body just posterior to the midline and near the upper end plate, very similar to the location of (L2-L3) of the synthetic spine model. Similarly, Liu et al.,[39] used combined dual fluoroscopic imaging system with MRI imaging techniques to investigate the dynamic flexion-extension motion of the lumbar spine in seven healthy human subjects doing a weight-lifting activity. The average CoR location for L4-L5 was near the back one-quarter of the disc and close to the posterior edge of the disc for L5-S1, which is comparable to what was found for the COR locations of the synthetic spine model at those spinal levels.

This research is not without limitations. The pure moment protocol used here was unable to match the 2000N axial load employed by Campbell et al.,[12] to analyze single motion segment units. A 20N axial load was applied to simply maintain compression on the spine for the duration of the pure moment testing method and only comparisons were made for flexion and extension. A sample size of one synthetic lumbar model was used for this testing, and no statistical analysis was performed on the outcomes. The likelihood of the mechanical properties of other models being similar is dependent on the manufacturer. Never-the-less, each model can serve as its control group if used to test multiple spinal instrumentation systems. Further, the model analyzed in this study will be used to develop a biomechanical testing protocol for assessing spinal orthoses, where a repeatable material with a physiological response is desired. Knowledge of the location of the global IAR is required as input information for the control strategy of the robotic testing platform.[15,26]

Conclusion

Tissue-based testing methods are recognized as the standard of practice for analyzing and comparing spinal instrumentation devices. However, there are many limitations with using human tissue that can impact the feasibility and study outcome that include, but are not limited to, cost, tissue quality, age, gender, and surgical or disease condition. Synthetic biomimetic models of the human body provide a cost effective alternative to cadaveric tissue that should overcome many of these limitations. This study determined the rotational and biomechanical stiffness properties of a full length synthetic lumbar spine model and found them to be comparable to *in vivo* and *in vitro* findings supporting its use as a viable alternative to cadaveric tissue. Additionally, a new mathematical approach was developed to calculate the CoR and IAR parameters using commonly measured spatial data of individual bodies moving in space. The technique was used to determine these kinematic parameters of CoR and IAR for the full length synthetic lumbar spine model and were also found to be comparable to *in vitro* and *in vivo* published findings further support its use other biomechanical studies of the lumbar spine. Future plans are to use the synthetic lumbar spine model as the foundation of a testing standard for biomechanically assessing, classifying, and ranking low back support devices, as the use of human cadaveric tissue is not feasible.

Acknowledgments

None.

Conflicts of interest

The authors declare there is no conflict of interest.

References

1. Gonzalez Blohm SA, Doulgeris JJ, Lee WE, et al. The current testing protocols for biomechanical evaluation of lumbar spinal implants in laboratory setting: A Review of the literature. *Biomedical Research International.* 2015:1–15.

2. Goel VK, Wilder DG, Pope MH, et al. Biomechanical testing of the spine. Load-controlled versus displacement-controlled analysis. *Spine.* 1995;20(21):2354–2357.

3. Panjabi MM, Oxland TR, Yamamoto I, et al. Mechanical behavior of the human lumbar and lumbosacral spine as shown by three-dimensional load-displacement curves. *The Journal of Bone and Joint Surgery.* 1994;76(3):413–424.

4. Patwardhan AG, Havey RM, Meade KP, et al. A follower load increases the load-carrying capacity of the lumbar spine in compression. *Spine*. 1999;24(10):1003–1009.

5. Panjabi MM. Hybrid multidirectional test method to evaluate spinal adjacent level effects. *Clinical Biomechanics*. 2007;22(3):257–265.

6. Kelly B. *A Multiaxis programmable spine robot for the study of multibody spinal biomechanics using real-time hybrid force and displacement control strategies*. Doctoral Dissertation. The University of Tennessee Health Science Center. 2005;7(3):56 p.

7. Stubbs, Jessica Rose. *Use of a multi-axis robotic testing platform to investigate the sagittal mechanics of the multi-body lumbar spine.* Theses and Dissertations (ETD). 2011. 256 p.

8. Campbell JR, Imsdahl S, Ching RP. *Evaluation of a synthetic functional spine unit*. Northwest Biomechanics Symposium. 2011.

9. Domann JP. *Development and validation of an analgoue lumbar spine model and its integral components.* Master's Thesis, University of Kansas. 2011.

10. Domann J, Mar D, Johnson A, et al. The analogue spine model: The first anatomically a mechanically correct synthetic physical model of the lumbar spine. *The Spine Journal.* 2011;11(10):S155–S156.

11. Wang T, Ball JR, Pelletier MH, et al. Initial experience with synthetic spinal motion segments: biomechanical assessment of high cycle and implant. Poster Presentation. *Orthopedic Research Society Meeting.* 2014;1(1):3.

12. Campbell JR, Imsdahl SI, Ching RP. Evaluation of a Synthetic L2-L5 Spine model for biomechanical testing. Poster Presentation. *Canadian Biomechanics Society.* 2012. 1 p.

13. Camisa W, Leasure JM, Buckley JM. *Biomechanical validation of a synthetic lumbar spine. Poster Presentation, 2014 Annual Meeting of the North American Spine Society*. 2015. 236 p.

14. Wang T, Ball JR, Pelletier MH, et al. Biomechanical evaluation of a biomimetic spinal construct. *J Exp Orthop*. 2014;1(1):3.

15. DiAngelo DJ, Hillyard DC. A novel distractive and mobility-enabling lumbar spinal orthosis. *Journal of Rehabilitation and Assistive Technologies Engineering*. 2016;3:1–10.

16. Cossette JW, Farfan HF, Robertson GH, et al. The instantaneous center of rotation of the third lumbar intervertebral joint. *J Biomech*. 1971;4(2):149–53.

17. Gertzbein SD, Holtby R, Tile M, et al. Determination of a locus of instantaneous centers of rotation of the lumbar disc by moiré fringes. A new technique. *Spine (Phila Pa 1976)*. 1984;9(4):409–413.

18. Haher TR, O'Brien M, Felmly WT, et al. Instantaneous axis of rotation as a function of three columns of the spine. *Spine (Phila Pa 1976)*. 1992;17(6 Suppl):S149–54.

19. Haughton VM, Rogers B, Meyerand ME, et al. Measuring the axial rotation of lumbar vertebrae *in vivo* with MR imaging. *AJNR Am J Neuroradiol*. 2002;23(7):1110–1116.

20. Inoue M, Mizuno T, Sakakibara T, et al. Trajectory of instantaneous axis of rotation in fixed lumbar spine with instrumentation. *J Orthop Surg Res*. 2017;16;12(1).

21. Pearcy MJ, Bogduk N. Instantaneous axes of rotation of the lumbar intervertebral joints. *Spine (Phila Pa 1976)*. 1988; 13(9):1033–1041.

22. Sakamaki T, Katoh S, Sairyo K. Normal and spondylolytic pediatric spine movements with reference to instantaneous axis of rotation. *Spine(Phila Pa 1976)*. 2002;27(2):141–145.

23. Sengupta DK, Demetropoulos CK, Herkowitz HN. Instant axis of rotation of L4-5 motion segment—a biomechanical study on cadaver lumbar spine. *J Indian Med Assoc*. 2011;109(6):389.

24. Xia Q, Wang S, Kozanek M, et al. In-vivo motion characteristics of lumbar vertebrae in sagittal and transverse planes. *J Biomech*. 2010;43:1905–1909.

25. Crisco JJ 3rd, Chen X, Panjabi MM, et al. Optimal marker placement for calculating the instantaneous center of rotation. *J Biomech*. 1994;27(9):1183–1187.

26. Kelly BP, DiAngelo DD. A Multiaxis Programmable Robot for the Study of Multibody Spine Biomechanics Using a Real-time Trajectory Path Modification Force and Displacement Control Strategy. *J Med Devices*. 2013;7(3):034502-034502–7.

27. Kelly BP, Zufelt NA, Sander EJ, et al. The influence of fixed sagittal plane centers of rotation on motion segment mechanics and range of motion in the cervical spine. *J Biomech*. 2013;46(7):1369–1375.

28. DiAngelo DJ, Foley KT, Morrow BP, et al. *In vitro* testing of lumbar disc arthroplasty devices. *The Open Spine Journal*. 2014;6: 9–25.

29. Salb KN, Wido DM, Stewart TE, et al. Development of a robotic assembly for analyzing the instantaneous axis of rotation of the foot ankle complex. *Applied Bionics and Biomechanics*. 2016;1–9.

30. Ahmadi A, Maroufi N, Behtash H, et al. Kinematic analysis of dynamic lumbar motion in patients with lumbar segmental instability using digital videofluoroscopy. *Eur Spine J*. 2009;18(11):1677–1685.

31. Dvorak J, Panjabi MM, Chang DG, et al. Functional radiographic diagnosis of the lumbar spine. Flexion-extension and lateral bending. *Spine (Phila Pa 1976)*. 1991;16(5):562–571.

32. Hayes MA, Howard TC, Gruel CR, et al. Roentgenographic evaluation of lumbar spine flexion-extension in asymptomatic individuals. *Spine (Phila Pa 1976)*. 1989;14(3):327–331.

33. Lee SW, Wong KW, Chan MK, et al. Development and validation of a new technique for assessing lumbar spine motion. *Spine (Phila Pa 1976)*. 2002;27(8):E215–20.

34. Pearcy M, Portek I, Shepherd J. Three-dimensional x-ray analysis of normal movement in the lumbar spine. *Spine (Phila Pa 1976)*. 1984;9(3):294–297.

35. White AA, Panjabi MM. Clinical biomechanics of the spine, 2nd ed. 1990, p. 86–113.

36. Panjabi MM. Mechanical behavior of the human lumbar and lumbosacral spine as shown by three-dimensional load-displacement curves. *The Journal of Bone and Joint Surgery*. 1994;76(3):413–424.

37. Yamamoto I. Three-dimensional movements of the whole lumbar spine and lumbosacral joint. *Spine 1989*. 14(11):1256–1260.

38. Bifulco P, Cesarelli M, Cerciello T, et al. A continuous description of intervertebral motion by means of spline interpolation of kinematic data extracted by videofluoroscopy. *J Biomech*. 2012;45(4):634–641.

39. Liu Z, Tsai TY, Wang S, et al. Sagittal plane rotation center of lower lumbar spine during a dynamic weight-lifting activity. *J Biomech*. 2016;49(3):371–375.